Available online at www.sciencedirect.com
SCIENCE DIRECT®
Acta Materialia 53 (2005) 1347–1359
Acta MATERIALIA
www.actamat-journals.com

Suppression of nanocrack generation in nanocrystalline materials under superplastic deformation

I.A. Ovid'ko *, A.G. Sheinerman

Institute for Problems of Mechanical Engineering, Russian Academy of Sciences, Bolshoj 61, Vas. Ostrov, St. Petersburg 199178, Russia

Received 5 February 2004; received in revised form 18 November 2004; accepted 19 November 2004
Available online 30 December 2004

Abstract

A theoretical model is suggested which describes the suppressing effect of grain boundary diffusion on the nanocrack generation in nanocrystalline materials under high strain rate superplastic deformation. In the framework of the model, grain boundary sliding intensively occurs in deformed nanocrystalline materials and causes the storage of grain boundary dislocations at triple junctions of grain boundaries. Relaxation of the stresses of these dislocations occurs via either the nanocrack generation or enhanced diffusional mass transfer in vicinities of triple junctions, depending on the material, structure and deformation parameters. If the former relaxation mechanism is dominant, nanocracks are intensively generated and converge giving rise to the brittle behavior of a nanocrystalline specimen. If the second relaxation mechanism is dominant, diffusion suppresses the nanocrack generation and thereby promotes superplastic deformation in a nanocrystalline material.

Keywords: Nanocrystalline materials; Grain boundaries; Mechanical properties; Fracture; Superplasticity

1. Introduction

High strain rate superplasticity (with the strain rate up to 10^{-2} s^{-1}) of nanocrystalline materials such as Ni_3Al, Al- and Ti-based alloys [1–8] is a remarkable phenomenon which is different from both superplasticity of microcrystalline solids and conventional low ductility of nanocrystalline materials. First of all, nanocrystalline materials commonly exhibit the superplastic behavior at higher strain rates and lower temperatures compared to their micro-grained counterparts. Also, high strain rate superplasticity in nanocrystalline materials is characterized by very high flow stresses and the essential strengthening at the extensive stage of deformation [1–8]. It is contrasted to superplasticity of microcrystalline materials, occurring at low flow stresses without pronounced strengthening [9]. In addition, most nanocrystalline materials show low ductility due to either brittle fracture or plastic flow localization (followed by necking) at low plastic strain [10–13]. In this context, recent experimental observations of high strain rate superplasticity [1–8] (and similar data on good ductility [14–17]) of nanocrystalline materials give exciting evidence for the unusual deformation behavior of such materials. This creates high interest in understanding the fundamentals of superplasticity in the nanocrystalline matter, motivated by a wide range of potential applications of simultaneously superplastic and superstrong nanocrystalline materials.

Following reviews [7,8] of experimental data on high strain rate superplasticity of nanocrystalline materials, grain boundary (GB) sliding is identified as the dominant mode of superplastic deformation in

* Corresponding author: Tel.: +7 812 321 4764; fax: +7 812 321 4771.
E-mail address: ovidko@def.ipme.ru (I.A. Ovid'ko).

1359-6454/$30.00
doi:10.1016/j.actamat.2004.11.026

such materials. Also, the lattice dislocation slip and rotational deformation mode (occurring via movement of GB disclinations and causing crystal lattice rotations in nanograins [18–23]) essentially contribute to superplastic deformation [7,8]. Based on these experimental data [7,8], a theoretical model [24,25] has been suggested describing the unusual strengthening in superplastic nanocrystalline materials as the phenomenon related to GB sliding which occurs via GB dislocation movement and leads to the storage of GB dislocations at triple junctions of GBs. In these circumstances, the GB storage provides the strengthening that prevents shear banding and thereby macroscopic necking followed by failure. On the other hand, the GB dislocation storage is capable of causing the stress concentration and consequent generation of nanocracks in the vicinities of triple junctions; see a theoretical model [26]. These theoretical representations account for experimental data [14] on observation of triple junction nanocracks in nanocrystalline Ni showing a good ductility. Triple junction nanocracks can be treated as nuclei of cracks that grow along GB planes and converge giving rise to macroscopic intergranular fracture often observed experimentally in nanocrystalline bulk materials and coatings [11,14]. In doing so, following a theoretical model [27] and molecular dynamics simulations [28], nucleation of triple junction nanocracks is enhanced near the tips of macroscopic cracks and thereby accelerates macroscopic crack propagation. Also, convergence of nanocracks growing along different GB planes is effectively described as a percolation process [29] resulting in the macroscopic intergranular fracture at a critical concentration of nanocracks in a mechanically loaded nanocrystalline specimen. Besides, as noted by Kumar et al. [11,14], triple junction nanocracks can serve as sites for nucleation of dimples experimentally observed at fracture surfaces in nanocrystalline materials. Thus, taking into account the experimental data [11,14], molecular dynamics simulations [28] and theoretical representations [26,27], triple junction nanocracks have been identified as the typical defects initiating macroscopic fracture processes in nanocrystalline matter. In this context, it is highly interesting to identify the mechanisms that are capable of suppressing the generation and growth of triple junction nanocracks in deformed nanocrystalline materials. In particular, such mechanisms are of crucial importance for understanding the fundamental nature of superplasticity, because the suppression of nanocrack generation is among the most important issues for superplastic flow. The main aim of this paper is to suggest a theoretical model describing the suppression of the generation and growth of triple junction nanocracks in deformed nanocrystalline materials as the phenomenon related to enhanced diffusion processes in GBs.

2. Grain boundary sliding and generation of nanocracks in deformed nanocrystalline materials

Let us consider a nanocrystalline solid under superplastic deformation occurring via both GB sliding (dominant mode) and conventional lattice dislocation slip. In the framework of our model, the combined action of these deformation mechanisms is realized as follows. In nanograins of the mechanically loaded material, lattice dislocations are generated and move towards GBs (Fig. 1(a)). The lattice dislocations are absorbed by GBs (Fig. 1(b)) where they split into GB dislocations (Fig. 1(c)). We assume that the splitting results in the formation of GB dislocations of two types: gliding and climbing GB dislocations with the Burgers vectors being parallel and perpendicular to the GB plane, respectively (Fig. 1(c)). The gliding dislocations move under the action of the external stress along GB planes towards triple junctions. At a certain level of the stress, the gliding dislocations reach triple junctions where they converge (Fig. 1(d)). As a result of this dislocation reaction, sessile dislocations are formed at triple junctions (Fig. 1(d)). With increasing plastic strain ε, the discussed process repeatedly occurs (Figs. 1(e)–(g)), in which case the Burgers vector magnitude B of the triple junction dislocation grows. At the same time, the triple junction dislocation elastically interacts with mobile GB dislocations gliding towards the triple junction. As shown in other papers [24,25], the elastic interaction hampers the GB dislocation movement (GB sliding) and thereby causes the strengthening of nanocrystalline materials. With increasing plastic strain degree ε, the dislocation reactions at a triple junction (Figs. 1(e)–(g)) give rise to a significant increase of the Burgers vector magnitude B of the triple junction dislocation. We suppose that, as a result of this process, B can reach large values being of the order of a nanometer or more (Fig. 1(g)). We will call triple junction dislocations with large Burgers vectors (Fig. 1(g)) superdislocations. The triple junction superdislocations create tensile stresses that are capable of inducing the formation of nanocracks in the vicinity of triple junctions (Fig. 1(h)) at some critical plastic strain [26].

Diffusion of atoms along GBs provides a partial relaxation of stress fields created by triple junction superdislocations. This relaxation gives rise to an increase of the critical plastic strain value at which triple junction nanocracks (Fig. 1(h)) are generated. In certain ranges of parameters of the system, GB diffusion is able to suppress the nanocrack generation near triple junctions during the extensive stage of plastic deformation. In the context discussed, we think that the diffusion-induced suppression of the nanocrack generation is very important for high strain rate superplasticity of the nanocrystalline matter. In order to reveal the conditions at which triple junction nanocracks (Fig. 1(h)) are gen-

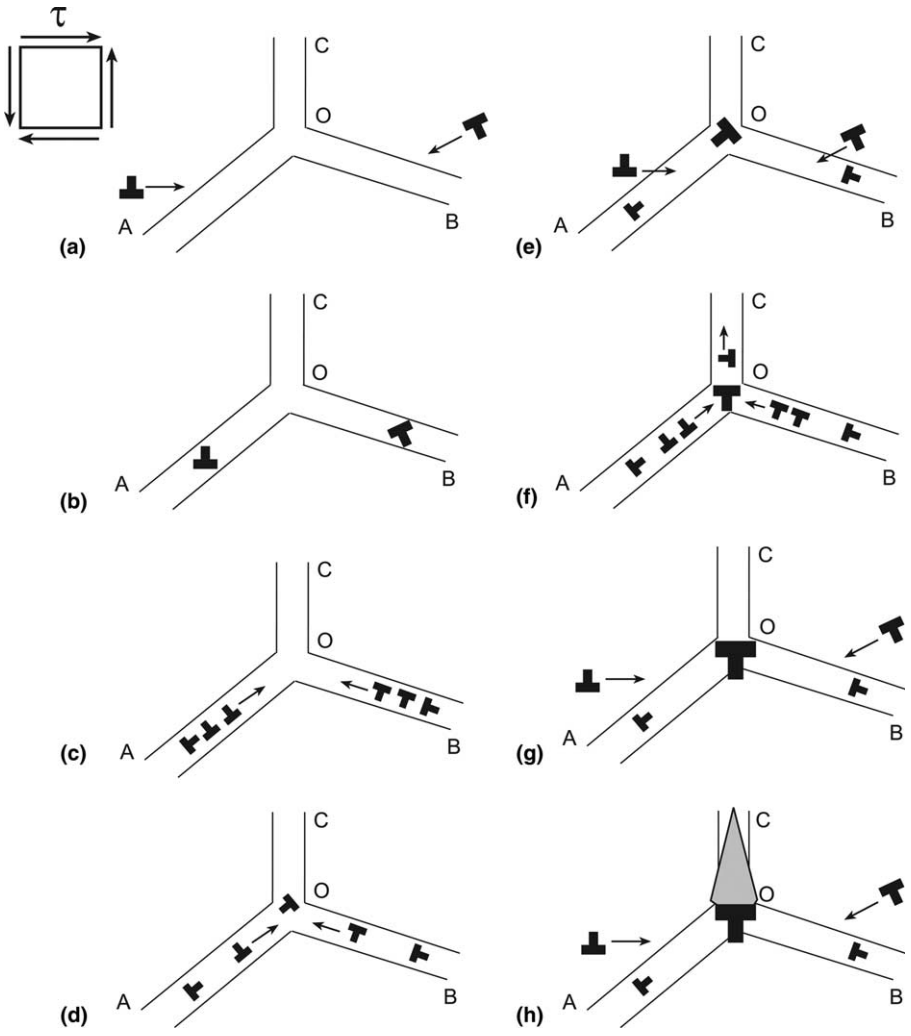

Fig. 1. Formation of superdislocation and nanocrack at triple junction of grain boundaries. (a) Lattice dislocations move under the external stress action towards grain boundaries. (b) Dislocations are trapped by boundaries. (c) Trapped dislocations split into gliding and climbing GB dislocations. Grain boundary dislocations in boundaries OA and OB glide towards triple junction O. (d) As a result of dislocation reaction, sessile dislocation is formed at triple junction O. (e), (f) and (g) Glide of new GB dislocations along boundaries OA and OB and their reactions at triple junction O leads to the formation of triple junction superdislocation. Triple junction superdislocation splits into dislocations that glide along boundary OC and sessile superdislocation that stays at triple junction O. (h) Nanocrack is generated in stress field created by sessile triple junction superdislocation.

erated in deformed nanocrystalline materials, we will describe in the next section the evolution of the superdislocation stresses which is governed by GB diffusion.

3. Diffusion-assisted relaxation of superdislocation stress field

Let us consider a triple junction superdislocation (Fig. 1(g)) whose stress field, in part, relaxes through diffusional mass transfer. The Burgers vector magnitude of the superdislocation is assumed to be constant. This corresponds to the "post-deformation situation" where the superdislocation is generated by the preceding plastic deformation and creates the stress field evolving in a nanocrystalline sample under no-loading conditions. It is hardly possible to analytically describe the diffusion-assisted evolution of the stress field of the triple junction superdislocation in time, because of the complicated geometry of a triple junction and adjacent GBs. In these circumstances, we will consider a simplified case of a superdislocation located in a flat GB (Fig. 2). This case reflects the key aspects of the problem and, at the same time, can be described in a convenient analytical way. So, we consider a model elastically isotropic infinite bicrystal containing a flat GB (Fig. 2). The dislocation-free boundary is characterized by a constant thickness δ_b (Fig. 2(a)). For the purposes of this paper, let us consider an edge (super)dislocation trapped by the boundary at the time moment $t = 0$ (Fig. 2(b)). In the coordinate system shown in Fig. 2, the center plane of the boundary coincides with the plane $y = 0$, the

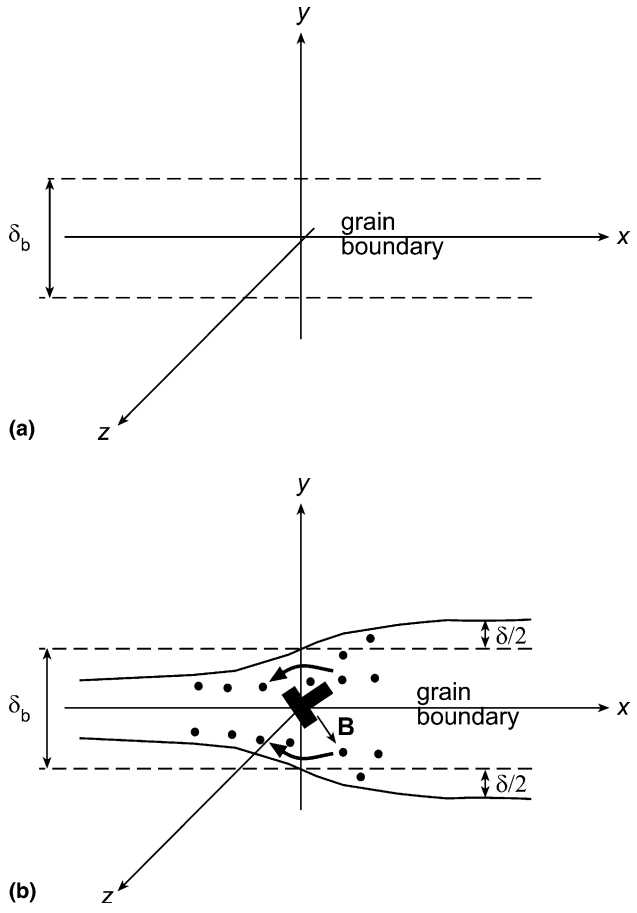

Fig. 2. Flat grain boundary in bicrystal. (a) Non-dislocated boundary. (b) Boundary contains dislocation whose stresses induce grain boundary diffusion and create elastic strains of adjacent grains.

dislocation line is located at the z-axis, and the dislocation Burgers vector $\mathbf{B} = B_x\mathbf{e}_x + B_y\mathbf{e}_y$ makes an arbitrary angle with the GB plane.

With the dislocation geometry shown in Fig. 2(b), the dislocation creates the tensile stresses capable of inducing the nucleation of a nanocrack along the GB segment located to the left of the dislocation. In this situation, details of both the stress distribution and vacancy transport in the half-space located to the right of the dislocation are not essential for a description of the nanocrack nucleation. This allows us to use the first approximation model of the system as a bicrystal and neglect the real triple junction geometry (Fig. 3(a)) with the two GBs located to the right of the dislocation. Also, consideration of the real situation, taking into account such details as GB non-planarity, GB character, GB misorientation and associated distribution of intrinsic GB dislocations, the presence of pile-ups of gliding GB dislocations, details of the (super)dislocation core, etc. (Fig. 3) is very cumbersome, sensitive to selection of many parameters, space-consuming and definitely beyond the scope of one paper. At the same time, these details can be treated as the second approximation ones whose account is not

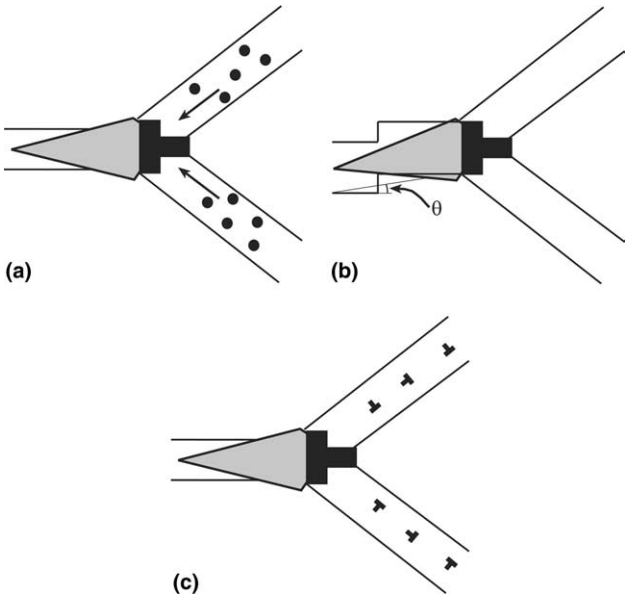

Fig. 3. Real triple junction and adjacent grain boundaries. (a) Nucleation of nanocrack near triple junction. (b) Nucleation of nanocrack along a grain boundary with a step. (c) Nucleation of nanocrack along a grain boundary containing gliding and intrinsic sessile boundary dislocations.

crucial for understanding the key aspects of diffusion-mediated suppression of nanocrack nucleation in deformed nanocrystalline materials.

For instance, the nanocrack slightly changes the direction of its growth at GB steps (Fig. 3(b)). In this case, besides the failure mode I (normal failure), which is realized in the case of a step-free, flat GB, the failure mode II (shear failure) contributes to the nanocrack growth along GB with steps. However, as shown by Gutkin and Ovid'ko [23], the contribution of the shear mode is proportional to $\sin\theta$, where θ is the angle between the GB plane with steps and the step-free GB plane. Steps provide very low values (several degrees) of the deviation angle θ (Fig. 3(b)) and thereby very weakly affect the nanocrack nucleation. The pile-ups of gliding GB dislocations consist of highly distant dislocations with small Burgers vector magnitudes of the order of 0.1 nm [30] (Fig. 3(c)). Also, intrinsic GB dislocations – carriers of GB type and misorientation – are characterized by Burgers vectors having magnitudes of around 0.1 nm [30] (Fig. 3(c)). In this situation, the effects of gliding and intrinsic GB dislocations on the nanocrack nucleation along a GB is negligibly low compared to that of the triple junction superdislocation having a Burgers vector magnitude of the order of 1 nm. The superdislocation core radius is of the order of 1 nm, too. In this case, the superdislocation core is localized at the triple junction and does not affect the nucleation of extended nanocrack (with the equilibrium length being around several nanometers; see Sections 4 and 5) along a GB segment adjacent to the triple junc-

tion. In the circumstances discussed, we will use the model system shown in Fig. 2(b) which allows us to effectively describe in the first approximation the role of GB diffusion processes in suppression of the nanocrack nucleation and growth in deformed nanocrystalline materials.

Let us designate the dislocation stress field created in the plate-like GB region as $\sigma_{jk}(x,t)$, where $j,k = x,y,z$. In the considered situation with an elastically isotropic bicrystal, the stress field components $\sigma_{jk}(x,0)$ at the initial time moment $t = 0$ are given by the following standard formulas [31]:

$$\sigma_{xx}(x,0) = \sigma_{yy}(x,0) = AB_y/x, \quad \sigma_{zz}(x,0) = 2\nu AB_y/x,$$
$$\sigma_{xy}(x,0) = AB_x/x, \quad \sigma_{xy}(x,0) = \sigma_{xz}(x,0) = \sigma_{yz}(x,0) = 0. \tag{1}$$

Here $A = G/[2\pi(1-\nu)]$, G is the shear modulus, and ν is the Poisson ratio. For $t > 0$, stress-driven diffusion processes occur causing a partial relaxation of the dislocation-induced stresses σ_{jk}.

Commonly, the GB diffusion coefficient D_b is larger by several orders than the bulk diffusion coefficient; see e.g. [30,32]. Therefore, in the framework of our model, we consider only fast diffusion occurring along GB. The stress relaxation effects of slow bulk diffusion will be neglected. The GB diffusion coefficient D_b is assumed to be constant in time. In these circumstances, in order to describe evolution of the dislocation stresses $\sigma_{jk}(x,t)$ in time, we will use the method suggested by Evans et al. [33] for the calculation of the stress concentration in the tip of a GB crack. Let $\delta(x,t)$ be a change of the GB thickness due to both the presence of the dislocation in the boundary and consequent diffusion induced by the dislocation stresses (Fig. 2(b)). Let J be the number of atoms diffusing along the GB plane $z = 0$ per both unit of time and unit of the GB width. Then, from the mass conservation law it follows that [33]

$$\Omega\frac{\partial J}{\partial x} + \frac{\partial \delta}{\partial t} = 0, \tag{2}$$

where Ω is the atomic volume. The linearized diffusion equation can be written as follows [33,34]:

$$\Omega J = -\frac{D_b\delta_b}{k_B T}\frac{\partial \mu}{\partial x}. \tag{3}$$

Here k_B denotes the Boltzmann constant, T the absolute temperature, and μ the chemical potential. The chemical potential is associated with the effects of the dislocation stress field, in which case it is written as $\mu = -\sigma\Omega$, where $\sigma = (\sigma_{xx} + \sigma_{yy} + \sigma_{zz})/3$. From formulas (2) and (3) one finds the following diffusion equation:

$$\frac{D_b\delta_b\Omega}{k_B T}\frac{\partial^2\sigma}{\partial x^2} + \frac{\partial \delta}{\partial t} = 0. \tag{4}$$

In order to describe evolution of the stresses $\sigma_{jk}(x,t)$, we should take into account that a change in the GB thickness due to the presence of the dislocation and stress-relaxing diffusion processes (Fig. 2(b)) induces elastic strains in the grains adjacent to the boundary. At the initial moment $t = 0$ the displacements u_y created by the dislocation [31] are symmetric about the GB plane $y = 0$, irrespective of the direction of the dislocation Burgers vector. As a result, these displacements are symmetric about the GB plane $x = 0$ at any time moment t. Therefore, the elastic displacements of the border lines between the GB region and adjacent grain interiors are equal to $\pm\delta/2$ (Fig. 2(b)). In other words, the change δ in the GB thickness is twice as large as each of the elastic displacements in question. In calculation of the stresses $\sigma_{jk}(x,t)$, for definiteness, we consider the upper grain adjacent to the boundary. The action of the stresses $\sigma_{jk}(x,t)$ at the border line between the upper grain and the GB is equivalent to that of distributed loads $q_j = -\sigma_{yj}$ (Fig. 4). The loads are given as: $q_y(x,t) = -\sigma_{yy}(x,t)$, $q_x(x,t) = -\sigma_{xy}(x,t)$, $-\infty < x < \infty$. These formulas allow us to find the expressions for the

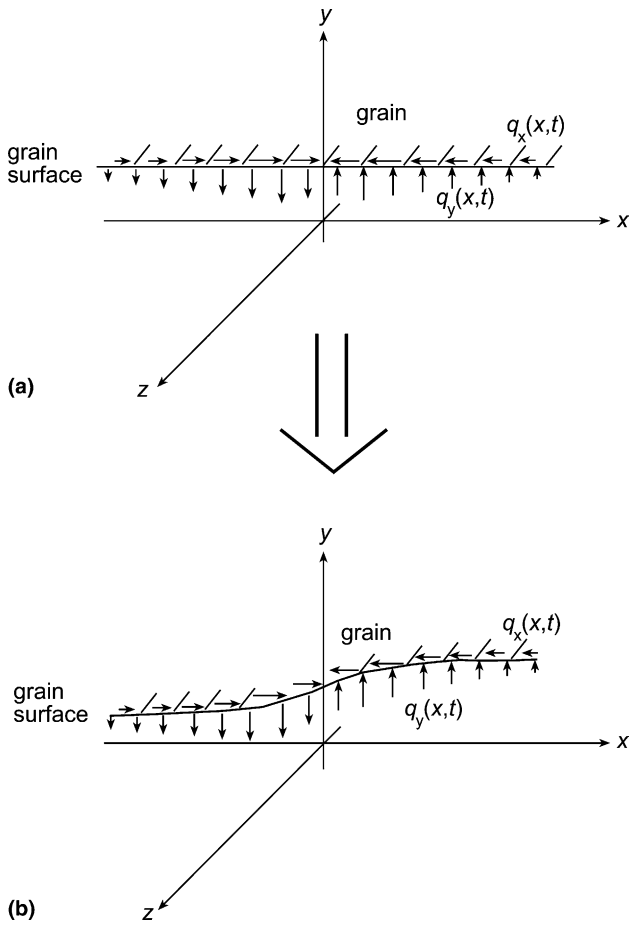

Fig. 4. Elastic strain of grain of bicrystal is created by surface loads $q_x(x,t)$ and $q_y(x,t)$ being equivalent to the dislocation stress field. (a) Non-strained state. (b) Strained state.

displacements, $u_x(x,t)$ and $u_y(x,t)$, of the border line. More precisely, these expressions can be found from the general formulas [35] for the displacements in a plane stress state and the standard replacement [35] $v \to v/(1-v)$ (at the same value of the shear modulus G) to obtain the plain strain displacements of interest. In doing so, we get:

$$u_x(x,t) = \frac{1-2v}{4G}\int_{-\infty}^{\infty} q_y(\psi,t)\,\mathrm{sign}(\psi - x)\,\mathrm{d}\psi - \frac{1-v}{\pi G}\int_{-\infty}^{\infty} q_x(\psi,t)\ln|\psi - x|\,\mathrm{d}\psi, \tag{5}$$

$$u_y(x,t) = -\frac{1-v}{\pi G}\int_{-\infty}^{\infty} q_y(\psi,t)\ln|\psi - x|\,\mathrm{d}\psi - \frac{1-2v}{4G}\int_{-\infty}^{\infty} q_x(\psi,t)\,\mathrm{sign}(\psi - x)\,\mathrm{d}\psi. \tag{6}$$

Following the approach of [33,36], we suppose that $\sigma_{yy}(x,t) = -q_y(x,t) = \int_{-\infty}^{\infty} C_1(\omega,t)\exp(\mathrm{i}\omega x)\,\mathrm{d}\omega$, $\sigma_{xy}(x,t) = -q_x(x,t) = \int_{-\infty}^{\infty} C_2(\omega,t)\exp(\mathrm{i}\omega x)\,\mathrm{d}\omega$, where $\mathrm{i} = \sqrt{-1}$. In these circumstances, from (5) and (6) we find:

$$u_x(x,t) = -\frac{1}{2G}\int_{-\infty}^{\infty}[\mathrm{i}(1-2v)C_1(\omega,t) + 2(1-v)C_2(\omega,t)\,\mathrm{sign}\ \omega]\frac{\exp(\mathrm{i}\omega x)}{\omega}\,\mathrm{d}\omega, \tag{7}$$

$$u_y(x,t) = -\frac{1}{2G}\int_{-\infty}^{\infty}[2(1-v)C_1(\omega,t)\,\mathrm{sign}\ \omega - \mathrm{i}(1-2v)C_2(\omega,t)]\frac{\exp(\mathrm{i}\omega x)}{\omega}\,\mathrm{d}\omega. \tag{8}$$

With expression (7) for u_x and the equation $\sigma_{yy} = \int_{-\infty}^{\infty} C_1(\omega,t)\exp(\mathrm{i}\omega x)\,\mathrm{d}\omega$ substituted into the relationship [35] $\partial u_x/\partial x = [1/(2G)][(1-v)\sigma_{xx} - v\sigma_{yy}]$, we find:

$$\sigma_{xx}(x,t) = \int_{-\infty}^{\infty}[C_1(\omega,t) - 2\mathrm{i}C_2(\omega,t)\,\mathrm{sign}\ \omega]\exp(\mathrm{i}\omega x)\,\mathrm{d}\omega. \tag{9}$$

Substitution of formula (9), the expression for σ_{yy} and relation $\sigma_{zz} = v(\sigma_{xx} + \sigma_{yy})$ to the definition $\sigma = (\sigma_{xx} + \sigma_{yy} + \sigma_{zz})/3$ gives

$$\sigma(x,t) = (2/3)(1+v)\int_{-\infty}^{\infty}[C_1(\omega,t) - \mathrm{i}C_2(\omega,t)\,\mathrm{sign}\ \omega]\exp(\mathrm{i}\omega x)\,\mathrm{d}\omega. \tag{10}$$

Account for the equality $\delta = 2u_y$ and substitution of the expressions for σ and δ into diffusion equation (4) yields:

$$C_1(\omega,t) = C_{10}\exp(-\alpha_1|\omega^3|t),\quad C_2(\omega,t) = C_{20}\exp(-\alpha_2|\omega^3|t), \tag{11}$$

where $\alpha_1 = (1+v)GD_b\delta_b\Omega/[3(1-v)k_BT]$ and $\alpha_2 = 2(1-v)\,\alpha_1/(1-2v)$. Inserting the first of formulae (11) into the relation

$$\sigma_{yy}(x,t) = \int_{-\infty}^{\infty} C_1(\omega,t)\exp(\mathrm{i}\omega x)\,\mathrm{d}\omega,$$

one obtains:

$$\sigma_{yy}(x,t) = \int_{-\infty}^{\infty} C_{10}(\omega)\exp(-\alpha_1|\omega^3|t)\exp(\mathrm{i}\omega x)\,\mathrm{d}\omega. \tag{12}$$

From formula (12) it follows that

$$\sigma_{yy}(x,0) = \int_{-\infty}^{\infty} C_{10}(\omega)\exp(\mathrm{i}\omega x)\,\mathrm{d}\omega. \tag{13}$$

The reverse Fourier transform of Eq. (13) results in:

$$C_{10}(\omega) = \frac{1}{2\pi}\int_{-\infty}^{\infty}\sigma_{yy}(x,0)\exp(-\mathrm{i}\omega x)\,\mathrm{d}x. \tag{14}$$

With the expression (1) $\sigma_{yy}(x,0) = AB_y/x$ substituted into formula (14), we have:

$$C_{10} = -\frac{\mathrm{i}AB_y}{2}\,\mathrm{sign}\ \omega. \tag{15}$$

Substitution of (15) into formula (12), with the replacement $\omega = p/(\alpha_1 t)^{1/3}$, yields:

$$\sigma_{yy}(x,t) = \frac{AB_y}{(\alpha_1 t)^{1/3}} f_1\left(x/(\alpha_1 t)^{1/3}\right), \tag{16}$$

where

$$f_1(\tilde{x}) = \int_0^{\infty} \mathrm{e}^{-p^3}\sin(p\tilde{x})\,\mathrm{d}p. \tag{17}$$

The function $f_1(\tilde{x})$ can also be presented in terms of generalized hypergeometric series.

The coefficient $C_{20}(\omega)$ and the stress $\sigma_{xy}(x,t)$ are obtained in the same fashion as the coefficient $C_{10}(\omega)$ and the stress $\sigma_{yy}(x,t)$ as follows:

$$C_{20}(\omega) = -\frac{\mathrm{i}AB_x}{2}\,\mathrm{sign}\ \omega, \tag{18}$$

$$\sigma_{xy}(x,t) = \frac{AB_x}{(\alpha_2 t)^{1/3}} f_1\left(x/(\alpha_2 t)^{1/3}\right). \tag{19}$$

Substitution of the expressions (15) and (18) for C_{10} and C_{20} to formula (9) yields the following expression for the stress $\sigma_{xx}(x,t)$:

$$\sigma_{xx}(x,t) = \frac{AB_y}{(\alpha_1 t)^{1/3}} f_1\left(x/(\alpha_1 t)^{1/3}\right) - \frac{AB_x}{(\alpha_2 t)^{1/3}} f_2\left(x/(\alpha_2 t)^{1/3}\right), \tag{20}$$

where

$$f_2(\tilde{x}) = 2\int_0^{\infty} \mathrm{e}^{-p^3}\cos(p\tilde{x})\,\mathrm{d}p. \tag{21}$$

The function $f_2(\tilde{x})$ can also be presented in terms of generalized hypergeometric series. In the limit as $t \to 0$ the stress $\sigma_{xx}(x,t)$, given by (20) and (21), satisfies the condition (1) $\sigma_{xx}(x,0) = AB_y/x$.

Thus, formulas (16), (17) and (19)–(21) describe the diffusion-assisted evolution of the superdislocation

stress field $\sigma_{jk}(x,t)$. The dependence $f_1(x/(\alpha_2 t)^{1/3}) = \sigma_{xy}(x,t)(\alpha_2 t)^{1/3}/(AB_x)$ figuring in formula (19) is presented in Fig. 5(a). The function $f_1(x/(\alpha_2 t)^{1/3})$ characterizes the dependence of the stress σ_{xy} on the coordinate x. As follows from formula (16), the x-dependence of the stress σ_{yy} is characterized by the function $f_1(x/(\alpha_1 t)^{1/3})$ and has the same character as the x-dependence of the stress σ_{xy}. As follows from Fig. 5(a), $f_1(0) = 0$ and, as a corollary, $\sigma_{xy}(x = 0,t) = \sigma_{yy}(x = 0,t) = 0$ at $t > 0$. So, GB diffusion removes singularities in the expressions for the dislocation stresses σ_{xy} and σ_{yy}, as with the previously analyzed case [33] of a GB crack.

The function $f_1(\tilde{x})$ has its maximum at $x = \tilde{x}_{\max} \approx 2.15$ and minimum at $\tilde{x} = \tilde{x}_{\min} \approx -2.15$. The maximum and minimum values of this function are $f_1(\tilde{x}_{\max}) \approx 0.586$ and $f_1(\tilde{x}_{\min}) \approx -0.586$, respectively. As a corollary, the stresses $\sigma_{yy}(x,t)$ and $\sigma_{xy}(x,t)$ have extreme points $x \approx \pm 2.15(\alpha_1 t)^{1/3}$ and $x \approx \pm 2.15(\alpha_2 t)^{1/3}$, respectively, at which their values are equal to $\pm 0.586AB_y/(\alpha_1 t)^{1/3}$ and $\pm 0.586AB_x/(\alpha_2 t)^{1/3}$, respectively. When the time t grows, the extreme points of the stresses $\sigma_{xy}(x,t)$ and $\sigma_{yy}(x,t)$ deviate from the dislocation line, and their magnitudes decrease.

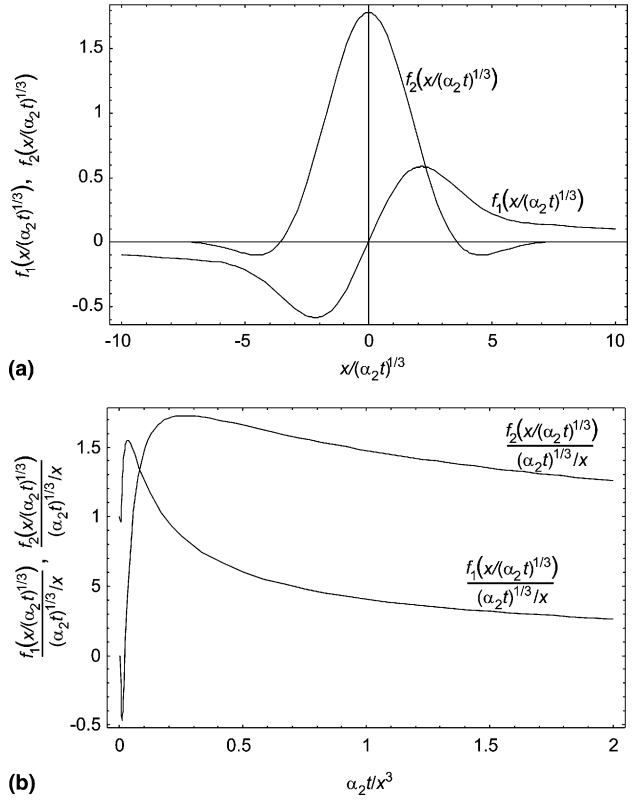

Fig. 5. (a) Dependences $f_1(x/(\alpha_2 t)^{1/3})$ and $f_2(x/(\alpha_2 t)^{1/3})$ which characterize the coordinate dependences of the stresses created by dislocation in flat grain boundary in bicrystal. (b) Dependences $(x/(\alpha_2 t)^{1/3})f_1(x/(\alpha_2 t)^{1/3})$ and $(x/(\alpha_2 t)^{1/3})f_2(x/(\alpha_2 t)^{1/3})$ which characterize the time dependences of the stresses created by dislocation in flat grain boundary in bicrystal.

The coordinate dependence of the stress σ_{xx} (see formula (20)) has a different character. Besides the term associated with the B_y-component of the dislocation Burgers vector, the stress σ_{xx} includes the term associated with the B_x-component of the dislocation Burgers vector, which is absent in the absence of GB diffusion. In particular, if $B_y = 0$, the stress σ_{xx} results from diffusion only and disappears if diffusion does not occur. In this case, the stress σ_{xx} originates from diffusion induced by the stress component σ_{xy}. In the case $B_y = 0$, the coordinate dependence of the stress σ_{xx} is characterized by the function $f_2(x/(\alpha_2 t)^{1/3})$ plotted in Fig. 5(a). As is seen in Fig. 5(a), the stress σ_{xx} has no singularity at $x = 0$ and oscillatory decreases with the distance $|x|$ from the dislocation line.

The time dependences of the dislocation stresses in the GB are presented in Fig. 5(b). This figure depicts the curves $(x/(\alpha_2 t)^{1/3})f_1(x/(\alpha_2 t)^{1/3}) = x\sigma_{xy}/(AB_x)$ and $(x/(\alpha_2 t)^{1/3})f_2(x/(\alpha_2 t)^{1/3}) = x\sigma_{xx}(B_y = 0)/(AB_x)$ vs. $\alpha_2 t/x^3$. As follows from Fig. 5(b), the dislocation stresses σ_{xy} and σ_{yy} first quickly decrease, then rapidly increase and slowly decrease. The stress $\sigma_{xx}(B_y = 0)$ first becomes negative (for $B_x > 0$), then changes its sign to positive, then rapidly grows in magnitude, and then slowly decreases with time. In the limit of $t \to +\infty$, all the dislocation stress components tend to zero, that is, diffusion provides a complete relaxation of the superdislocation stresses in the GB region.

4. Diffusion and nanocrack generation in vicinity of superdislocation with constant Burgers vector

In order to quantitatively characterize the nanocrack generation induced by the superdislocation stress field, we will calculate in the first approximation the equilibrium length l_e of the nanocrack. In doing so, with the results of the previous section, we will take into account relaxation of the superdislocation stresses due to diffusional mass transfer in the vicinity of the superdislocation. The Burgers vector magnitude B is assumed to be constant. That is, we consider the "post-deformation situation". (The nanocrack generation in vicinity of a superdislocation with the Burgers vector magnitude B growing in time will be considered in Section 5.)

The equilibrium length l_e of the nanocrack (Fig. 2(b)) is defined as that corresponding to the minimum or maximum energy of the system. If the system energy has a minimum, the equilibrium of the nanocrack is stable, whereas if it has a maximum, the equilibrium is unstable. In calculation of l_e, we will use the configurational force method [37] effectively exploited in analysis of the generation of plane microcracks in the stress fields of superdislocations [26,37], dislocation pile-ups [37], disclination loops [38], lamellar terminations in eutectics [39] and wedge disclinations [23,40]. Following [37], the

configurational force F is defined as the elastic energy released when a crack moves over a unit distance. In the situation with the plane strain state of an elastically isotropic solid, examined in this paper, F can be written in its general form as follows [37]:

$$F = \frac{\pi(1-\nu)l}{4G}\left(\bar{\sigma}_{yy}^2 + \bar{\sigma}_{xy}^2\right), \tag{22}$$

where $\bar{\sigma}_{yy}$ and $\bar{\sigma}_{xy}$ are the mean weighted values of stress tensor components σ_{yy} and σ_{xy}, respectively. These weighted stress tensor components are calculated using the following formula [37]:

$$\bar{\sigma}_{my}(l,t) = \frac{2}{\pi l}\int_0^l \sigma_{my}(x,t)\sqrt{\frac{x}{l-x}}\,\mathrm{d}x, \quad m = x,y. \tag{23}$$

The equilibrium length l_e of the nanocrack is derived from the balance $F(l = l_e) = 2\gamma_e$ between a release F of the elastic energy and the formation of two new nanocrack surfaces characterized by the surface energy density γ_e per unit area. Here $\gamma_e = \gamma_s - \gamma_b/2$, where γ_s is the specific surface energy and γ_b is the specific energy of the GB per unit area of its plane. The nucleation of the nanocrack (Fig. 1(b)) is energetically favorable, if $F > 2\gamma_e$, and unfavorable, if $F < 2\gamma_e$.

In the following we suppose that the dislocation Burgers vector is perpendicular to the GB plane and has the form $\mathbf{B} = -B\mathbf{e}_y$. As follows from formula (19), for such a dislocation $\sigma_{xy}(x,t) \equiv 0$. Therefore, we have: $\bar{\sigma}_{xy} \equiv 0$. In order to calculate $\bar{\sigma}_{yy}$, we represent the factor $\sin p\tilde{x}$ in the expression (17) for $f_1(\tilde{x})$ as a power series: $\sin p\tilde{x} = \sum_{n=0}^{\infty}(-1)^n\frac{(p\tilde{x})^{2n+1}}{(2n+1)!}$. Substitution of the latter equality into formula (17) and its integration yield:

$$f(\tilde{x}) = \frac{1}{3}\sum_{n=0}^{\infty}(-1)^n\frac{\Gamma[(2n+2)/3]}{(2n+1)!}\tilde{x}^{2n+1}, \tag{24}$$

with $\Gamma(u)$ being the gamma function. With $m = y$, substitution of (16) and (24) into formula (23) and consequent integration in this formula yield: $\bar{\sigma}_{yy}(l,t) = -(AB/l)\,g(l/(\alpha t)^{1/3})$, where

$$g(p) = -\frac{2}{3}\sum_{n=0}^{\infty}\frac{\Gamma[(2n+2)/3](4n+4)!}{(2n+1)![(2n+2)!]^2}\left(-\frac{p^2}{16}\right)^{n+1}. \tag{25}$$

The function $g(p)$ can also be represented through generalized hypergeometric series. For large values of $p(p \geqslant 20)$, the direct calculation of the function $g(p)$ in accordance with formula (25) is complicated. In this situation, it is convenient to use the asymptotic representation $g(p \to \infty) \approx 2 - 0.90p^{-1/2}$.

After substitution of formula (22), expression for $\bar{\sigma}_{yy}$, equations $\bar{\sigma}_{xy} = 0$ and $A = G/[2\pi(1-\nu)]$ into the condition $F(l = l_e) = 2\gamma_e$, we find the following equation for the equilibrium length of a nanocrack:

$$Q(l_e/b, Z) = \kappa. \tag{26}$$

Here $Q(p,Z) = (1/p)g^2(p/Z)$, $\kappa = 32\,\pi(1-\nu)\gamma_e/(GB)$, and $Z = (\alpha t)^{1/3}/B$.

The dependences $Q(l/B,Z)$ are presented in Fig. 6, for various values of parameter Z characterizing the diffusion-assisted relaxation of the superdislocation stresses. Also, for comparison, dashed curve 1 in Fig. 6 shows the values of $Q(l/B,Z)$ at $Z = 0$, corresponding to the situation where diffusion is absent. The horizontal line in Fig. 6 shows the value of the parameter κ ($\kappa \approx 0.6$) in the case of $B = 2$ nm, for nanocrystalline Ni characterized by the following averaged values of parameters: $\gamma_s = 1.725$ J/m^2 [31], $\gamma_b = 0.69$ J/m^2 [31], $G = 0.79 \times 10^{11}$ Pa [41], and $\nu = 0.31$ [41]. Growth of the nanocrack is energetically favorable, if $Q(l/B,Z) > \kappa$.

With this criterion, for $Z > 0$, we distinguish the following two cases, depending on the relationship between κ and Z:

(i) The horizontal line $\kappa = 0.6$ intersects the curve $Q(l/B,Z)$ at two points, $l/B = l_{e1}/B$ and $l/B = l_{e2}/B$ ($l_{e1} < l_{e2}$), which correspond to the equilibrium lengths of the nanocrack $l = l_{e1}$ and $l = l_{e2}$, respectively (see curves b and c in Fig. 6, respectively). (For definiteness, the lengths l_{e1} and l_{e2} are shown in Fig. 6, for the parameter values corresponding to curve c).

(ii) The horizontal line $\kappa = 0.6$ lies above the curve $Q(l/B,Z)$ and does not intersect it (see curve d in Fig. 6).

The situation (i) is realized when the maximum of the curve $Q(l/B,Z)$ is higher than κ and thereby the maximum value of the function $ZQ(l/B,Z)$ is larger than κZ. Since $Q(l/B,Z) = (B/l)\;g^2(l/(BZ))$, the equation $ZQ(l/B,Z) = g^2(l/(BZ))/[l/(BZ)]$ is valid. As a corollary, $ZQ(l/B,Z)$ represents a function of the sole argument $l/(BZ)$. Numerical estimates show that the maximum of this function is about 0.83. Therefore, the situation (i) comes into play, if $\kappa Z < 0.83$.

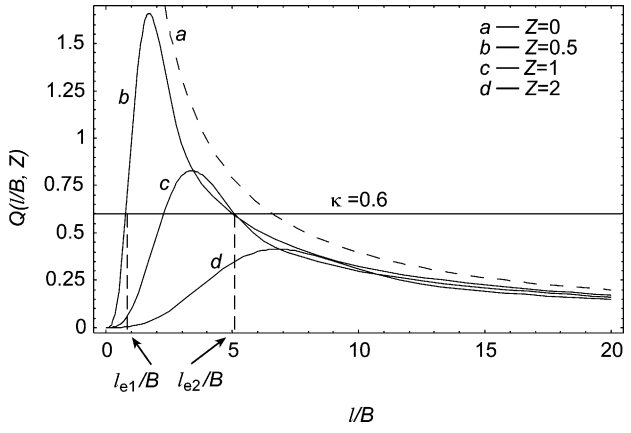

Fig. 6. Dependences $Q(l/B,Z)$. Horizontal line shows value of parameter κ. Nanocrack growth is suppressed (energetically unfavorable) if $Q(l/B,Z) < \kappa$.

The nanocrack growth is energetically favorable, provided $Q(l/B,Z) > \kappa$. As a consequence, in the situation (i), a decrease of the nanocrack length is energetically favorable, if either $l < l_{e1}$ or $l > l_{e2}$, and unfavorable, if $l_{e1} < l < l_{e2}$. Thus, the equilibrium of a nanocrack with the length $l = l_{e1}$ is unstable, while the equilibrium of a nanocrack with the length $l = l_{e2}$ is stable. In order to form a stable nanocrack with the length $l = l_{e2}$, the system should overcome an energetic barrier. The nanocrack nucleus should grow with the help of thermal fluctuations until its length l reaches the value of l_{e1}. Then its athermal growth until the state with $l = l_{e2}$ becomes energetically favorable. Further growth of a nanocrack (extension of the nanocrack to the range of $l > l_{e2}$) is energetically unfavorable. With increasing time t, the parameter Z increases, and the range $l_{e1} < l < l_{e2}$, in which the nanocrack growth is favorable, decreases (see curves 2 and 3 in Fig. 6). This tendency reflects the effect of GB diffusion providing a partial relaxation of the superdislocation stresses.

For $\kappa Z > 0.83$, the situation (ii) is realized in which the horizontal line $\kappa = 0.6$ lies above the curve $Q(l/B,Z)$ (see curve d in Fig. 6). In this situation, growth of a nanocrack in GB is energetically unfavorable at any values of l. That is, the nanocrack generation is completely suppressed by diffusion, for given constant value ($B = 2$ nm) of the superdislocation Burgers vector magnitude.

For comparison, dashed curve a in Fig. 6 illustrates the situation (iii) where diffusion is absent ($Z = 0$). In this situation, examined in detail in paper [26], $l_{e1} = 0$ $Q(l/B,Z) > \kappa$ when $l < l_{e2}$. In the situation (iii), the nanocrack nucleus athermally grows until its length l reaches the value of l_{e2}. In other words, when diffusion is absent or negligibly small, the system quickly reaches in a nonbarrier way its stable state with a triple junction nanocrack of the length l_{e2}. In order to generate the nanocrack, the system does not need to overcome any energetic barrier, in contrast to the situation (i). Also, the situation (iii) is contrasted to the situation (ii) where the nanocrack generation is completely suppressed by diffusion.

Thus, the GB diffusion provides the suppressing effect on the nanocrack generation near triple junctions containing superdislocations with constant Burgers vectors. The suppressing effect exhibits itself in a pronounced way in nanocrystalline materials with high diffusivity.

5. Nanocrack generation in vicinity of superdislocation with Burgers vector growing in time

Let us consider the formation of a triple junction nanocrack in the vicinity of a superdislocation whose Burgers vector magnitude B grows in time due to GB sliding (Fig. 1). Such processes of the nanocrack formation at triple junctions occur intensively during (super)plastic deformation of nanocrystalline materials; see experimental data [14] and theoretical model [26]. In the situation discussed, GB sliding causes an increase of the superdislocation Burgers vector magnitude B and thereby enhances the nanocrack formation. At the same time, GB diffusion provides a partial relaxation of the superdislocation stresses and, thus, hampers the nanocrack formation.

It is hardly possible to analytically calculate the equilibrium length of a nanocrack (Fig. 1(h)) in the stress field of the triple junction superdislocation. Therefore, in this paper, the stress field of the triple junction superdislocation will be approximated as that of a superdislocation at a flat GB in a bicrystal (Fig. 2(b)). Now let us turn to a description of evolution of Burgers vectors that characterize triple junction superdislocations in deformed nanocrystalline materials. As noted above, GB sliding through triple junctions in nanocrystalline materials under high strain rate superplastic deformation causes the Burgers vectors of triple junction dislocations to grow with rising time t (or plastic strain degree $\varepsilon = \dot{\varepsilon}t$, with plastic strain rate $\dot{\varepsilon}$ being constant) (Fig. 1) [24,25]. In the first approximation, we assume that the Burgers vector magnitude B characterizing the triple junction dislocation runs parallel with the time t (or plastic strain degree ε): $B = \beta t = \beta\varepsilon/\dot{\varepsilon}$, where β is a constant parameter. Then the stress $\sigma^s_{yy}(x,t)$ created by the superdislocation near the triple junction can be represented as the superposition of the stresses $\mathrm{d}\sigma_{yy}(x,\ t-t')$ created at the time moment t' by the triple junction dislocations with the infinitesimal Burgers vectors $\mathrm{d}B(t') = \beta\,\mathrm{d}t'$. Such dislocations are formed during the time interval from t' to $t' + \mathrm{d}t'$. Their stress field $\mathrm{d}\sigma_{yy}(x,t-t')$ is given by formula (16), with t and B being replaced by $t - t'$ and $\mathrm{d}B(t')$, respectively. That is, $d\sigma_{yy}(x,t-t') = \mathrm{d}B(t')\sigma_{yy}(x,t-t')|_{B=1}$. Thus, we have:

$$\sigma^s_{yy}(x,t) = \beta\int_0^t \mathrm{d}t'\sigma_{yy}(x,t-t')|_{B=1}. \tag{27}$$

With the left- and right-hand sides of formula (27) multiplied by the factor $[2/(\pi l)]\sqrt{x/(l-x)}$, after integration over x from 0 to l, we get:

$$\bar{\sigma}^s_{yy}(l,t) = \beta\int_0^t \mathrm{d}t'\bar{\sigma}_{yy}(l,t-t')|_{B=1}. \tag{28}$$

Here $\bar{\sigma}^s_{yy}(l,t)$ and $\bar{\sigma}_{yy}(l,t-t')$ are the mean weighted values of the stresses $\sigma^s_{yy}(x,t)$ and $\sigma_{yy}(x,t-t')$, respectively, in which case $\bar{\sigma}^s_{yy}(l,t) = [2/(\pi l)]\int_0^l \sigma^s_{yy}(x,t)\sqrt{x/(l-x)}\,\mathrm{d}x$, and $\bar{\sigma}_{yy}(l,t-t')$ is given by both the expression $\bar{\sigma}_{yy}(l,t-t') = -(AB/l)g[l/(\alpha^{1/3}(t-t')^{1/3})]$ and formula (25). After substitution of the expression for $\sigma_{yy}(l,t-t')$ into formula (28) and replacement of variables, $s = (t-t')/t$ and $\tau = \beta t/b$ (with b being the Burgers vector magnitude that characterizes an elementary gliding GB dislocation), we find:

$$\bar{\sigma}^{s}_{yy}(l,t) = -\frac{A\tau}{l/b} I(l/b, Z'\tau). \quad (29)$$

Here

$$I(p,v) = \int_0^1 g\left(\frac{p}{s^{1/3}v^{1/3}}\right) \mathrm{d}s \quad (30)$$

and $Z' = \alpha/(\beta b^2)$. As a result, we have the expression for σ^{s}_{yy}, which allows us to find the equation for the equilibrium length $l = l'_e$ of a nanocrack generated in the stress field of the triple junction superdislocation with a growing (in time) Burgers vector. This equation can be found in the same way as Eq. (26) (describing the equilibrium length $l = l_e$ of a nanocrack generated in the stress field of the dislocation with a constant Burgers vector) is obtained from the expression for $\bar{\sigma}_{yy}$. In doing so, after some algebra, we get the equation for l'_e:

$$Q'(l'_e/b) = \kappa', \quad (31)$$

where $Q'(p) = \tau^2 I^2(p,Z'\tau)/p$, and $\kappa' = 32\pi(1-\nu)\gamma_e/(Gb)$.

The dependences $Q'(l/b)$ are presented in Fig. 7, for different values of τ (Fig. 7(a)) and Z' (Fig. 7(b)). The horizontal lines show the value of the parameter κ' ($\kappa' = 12$). This value corresponds to the values of γ_s, γ_b, G and ν for nanocrystalline Ni (see above) and to the magnitude $b = 0.1$ nm of elementary Burgers vectors that characterize the gliding GB dislocations. Growth of the nanocrack is energetically favorable, if $Q'(l/b) > \kappa'$. As with the nanocrack generated in the stress field of a superdislocation with a constant Burgers vector (see Fig. 6), there are the following situations: for $Z' > 0$, the nanocrack growth in the stress field of a triple junction superdislocation with a growing Burgers vector is either energetically favorable in the range $l'_{e1} < l < l'_{e2}$ (see curves b and c in Figs. 7(a) and (b)) or unfavorable at any value of the nanocrack length l (see curve 1 in Fig. 7(a) and curve d in Fig. 7(b)). In the idealized case with $Z' = 0$ (dashed curve in Fig. 7(b)), where diffusion is absent, the nanocrack is characterized by one equilibrium length l'_{e2} (whereas $l'_{e1} = 0$). In this case, the nanocrack growth is energetically favorable, if $l < l'_{e2}$, and unfavorable, if $l > l'_{e2}$.

Let us describe the behavior characteristics (in particular, the equilibrium lengths l'_{e1} and l'_{e2}) of nanocracks as functions of the following parameters measured and controlled in experiments: plastic strain ε, plastic strain rate $\dot{\varepsilon}$ and temperature T. To do so, we should express parameters τ and $Z'\tau$ (figuring in formula for $Q'(p)$) through ε, $\dot{\varepsilon}$ and T. In the framework of our model, the Burgers vector magnitude B (that characterizes the triple junction superdislocation) grows due to GB sliding which occurs via movement of GB dislocations and their convergence at triple junctions (Fig. 1). In these circumstances, as shown in [25], the mean number n of dislocation convergence reactions at a triple junction is in the following approximate relationship with

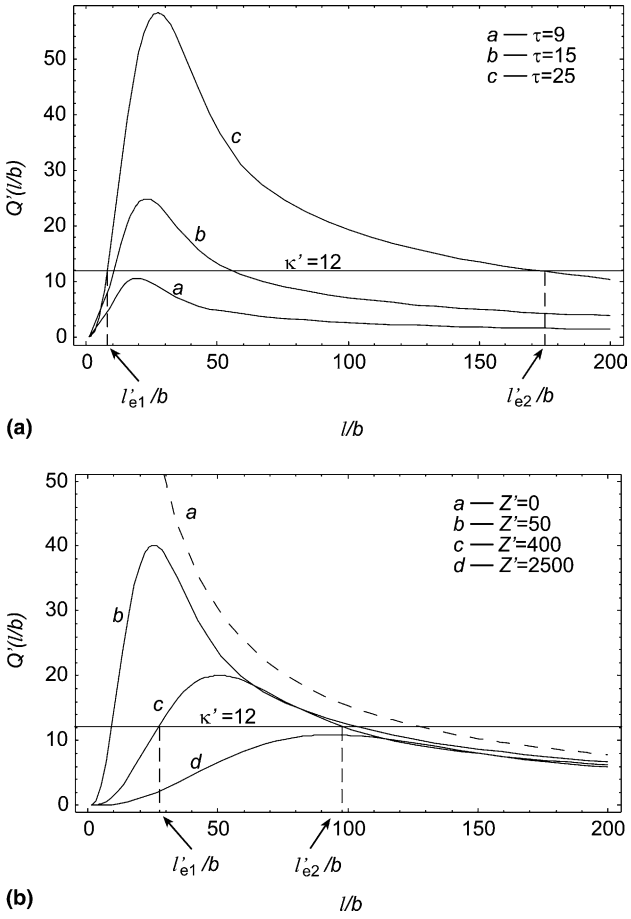

Fig. 7. Dependences $Q'(l/b)$, for the following values of parameters: (a) $Z' = 50$; (b) $\tau = 20$. Horizontal lines show value of parameter κ'. Nanocrack growth is suppressed (energetically unfavorable), if $Q'(l/b) < \kappa'$.

plastic strain ε_{GB} conducted by GB sliding in a deformed nanocrystalline sample: $n = 500\varepsilon_{GB}$, where $\varepsilon_{GB} = 0.5\varepsilon - 0.7\varepsilon$. At the same time, the Burgers vector magnitude B of the triple junction superdislocation (Fig. 1) is related to n as follows [25]: $B = \beta_0 nb$, where $\beta_0 = 0.1$–0.8 is the factor taking into account the triple junction geometry. With this formula substituted into the expression $\tau = \beta t/b = B/b$, we find: $\tau = 500\beta_0\ \varepsilon_{GB}$. For definiteness, we suppose that $\beta_0 = 0.5$ and $\varepsilon_{GB} = 0.5\varepsilon$, in which case τ is expressed through ε as follows: $\tau = 125\varepsilon$.

Now let us express the parameter $Z'\tau$ (figuring in the formula for $Q'(p)$) through ε, $\dot{\varepsilon}$ and T. From the definitions of the parameters τ, Z' and α ($\tau = \beta t/b$, $Z' = \alpha/(\beta b^2)$, and $\alpha = (1+\nu)GD_b\delta_b\Omega/[3(1-\nu)k_BT]$, respectively) as well as formula [30] $D_b = D_{b0}\exp[-Q_b/(RT)]$, we find: $\tau Z' = (1+\nu)GD_{b0}\delta_b \exp[-Q_b/(RT)]\Omega\varepsilon/[3(1-\nu)\dot{\varepsilon}b^3k_BT]$. This expression and the relationship $\tau = 125\varepsilon$ allow us to calculate $Q'(l'_e/b)$ (figuring in Eq. (31)) and the equilibrium lengths $l'_e = l'_{e1}$ and $l'_e = l'_{e2}$ (being solutions of Eq. (31)) as functions of the parameters ε, $\dot{\varepsilon}$ and T.

The calculated dependences of the non-dimensional equilibrium lengths l'_{e1}/b and l'_{e2}/b on plastic strain ε are presented in Fig. 8, for various values of parameters $\dot{\varepsilon}$ and T as well as the following values of parameters that characterize nanocrystalline Ni: $\gamma_s = 1.725$ J/m^2 and $\gamma_b = 0.69$ J/m^2 [31], $G = 0.79 \times 10^{11}$ Pa, $\nu = 0.31$, and $\Omega = 1.094 \times 10^{-29}$ m^{-3} [41], $D_{b0} = 1.75 \times 10^{-6}$ m^2 c^{-1} and $Q_b = 110$ kJ/mol [41,42]. The dependences of l'_{e1}/b and l'_{e2}/b on plastic strain ε are shown as, respectively, falling and rising curves in Fig. 8. For the same values of parameters $\dot{\varepsilon}$ and T, these dependences originate from the same point corresponding to a critical plastic strain ε'_0 (see Fig. 8). For $\varepsilon < \varepsilon'_0$, the nanocrack growth is unfavorable for any nanocrack length. For $\varepsilon > \varepsilon'_0$, the growth of a triple junction nanocrack becomes energetically favorable in the nanocrack length interval $l'_{e1} < l < l'_{e2}$. In this situation, in order to form a stable nanocrack with the length $l = l'_{e2}$, the system should overcome an energetic barrier. The nanocrack nucleus should grow with the help of thermal fluctuations until its length l reaches the value of l'_{e1}. Then its athermal growth until the state with $l = l'_{e2}$ becomes energetically favorable. Further growth of the nanocrack is forbidden.

As follows from Fig. 8, when plastic strain $\varepsilon(> \varepsilon'_0)$ increases, so does the equilibrium length l'_{e2}, while the equilibrium length l'_{e1} decreases. The first equilibrium length l'_{e1} is weakly sensitive to the parameters $\dot{\varepsilon}$ and T, in contrast to the second equilibrium length l'_{e2} which exhibits a significant growth with rising T and decreasing $\dot{\varepsilon}$.

Also, as it is evident from Fig. 8, the first equilibrium length l'_{e1} at temperature $T \geqslant 550$ K is rather high ($l'_{e1} > 100b = 10$ nm), even for high values of plastic strain rate and plastic strain ($\dot{\varepsilon} = 10^{-2}$ c^{-1} and $\varepsilon = 0.5$, respectively). At the same time, the thermally activated generation of a nanocrack with a large length $l'_{e1} > 100b = 10$ nm is hardly possible. It is indicative of effective diffusion-induced suppression of the nanocrack generation in deformed nanocrystalline Ni at $T \geqslant 550$ K. This phenomenon also comes into play in other nanocrystalline materials in certain ranges of their parameters, temperature and parameters of mechanical loading. It is of high importance for high strain rate superplasticity exhibited by the nanocrystalline matter.

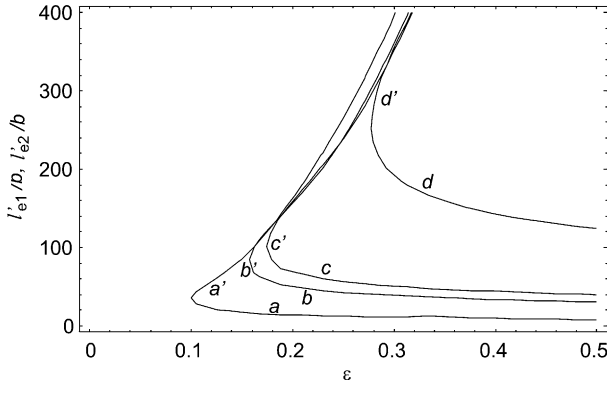

Fig. 8. Dependences of the non-dimensional equilibrium lengths l'_{e1}/b (falling curves a, b, c and d) and l'_{e2}/b (rising curves a', b', c' and d') on plastic strain ε, for the following values of parameters: $T = 450$ K, $\dot{\varepsilon} = 10^{-2}$ c^{-1} (curves a and a'); $T = 450$ K, $\dot{\varepsilon} = 10^{-3}$ c^{-1} (curves b and b'); $T = 500$ K, $\dot{\varepsilon} = 10^{-2}$ c^{-1} (curves c and c'); and $T = 550$ K, $\dot{\varepsilon} = 10^{-2}$ c^{-1} (curves d and d').

6. Concluding remarks

In this paper, it has been theoretically revealed that the generation of nanocracks in nanocrystalline materials can be effectively suppressed due to the stress relaxation effect of GB diffusion. Triple junction nanocracks – typical defects experimentally observed by Kumar et al. [14] in deformed nanocrystalline Ni – have been theoretically analyzed in detail. Such nanocracks are generated in the stress fields of superdislocations formed at triple junctions as a result of GB sliding along adjacent GB planes. Enhanced GB diffusion processes provide a partial relaxation of triple junction dislocation stresses and thereby hamper or even completely suppress the nanocrack generation at triple junctions during the extensive stage of (super)plastic deformation in nanocrystalline materials.

Thus, in nanocrystalline materials in which GB sliding essentially contributes to plastic flow, there is a competition between the two key factors affecting the nanocrack generation. The first factor is GB-sliding-induced storage of superdislocations at triple junctions, which enhances the nanocrack generation and growth. The second factor is the GB-diffusion-mediated relaxation of the superdislocation stresses, which hampers the nanocrack generation. At the first stage of plastic deformation, the superdislocation Burgers vectors are small, and thereby the driving force for the nanocrack generation at triple junctions is low. With rising plastic strain degree ε, the superdislocation Burgers vectors grow. At some critical value ε'_0 of plastic strain, the storage of superdislocations at triple junctions becomes sufficient to cause the intense generation of triple junction nanocracks. The critical plastic strain ε'_0 is small at high enough values of plastic strain rate $\dot{\varepsilon}$ and sufficiently low temperature T. In these circumstances, nanocrystalline materials show brittle behavior. However, for relatively small values of $\dot{\varepsilon}$ and high enough temperature T, the critical plastic strain ε'_0 is large (see e.g. curves 4 and 4′ in Fig. 8). That is, during the extensive stage of (super)plastic deformation, the stress relaxation effect of GB diffusion is dominant, which causes suppression of the nanocrack generation. Generally speaking, despite suppression of the nanocrack generation, failure processes in nanocrystalline materials can occur through

shear banding and macroscopic necking [43]. Therefore, nanocrystalline materials show superplasticity, if both the nanocrack generation and shear banding are simultaneously suppressed during the extensive stage of plastic deformation.

Lattice dislocation slip and GB sliding have been experimentally identified as dominant deformation modes in nanocrystalline materials exhibiting a substantial ductility [14] and superplasticity [6–8]; see also theoretical models [44–46]. This corresponds to the key statements of our model, based on the idea of interaction between lattice dislocation slip, GB sliding, GB diffusion, and failure processes. So, the lattice dislocation slip supplies lattice dislocations to GBs where they split into climbing and gliding GB dislocations (Fig. 1). The climbing GB dislocations move to new positions and annihilate, in which case they emit point defects and cause GB diffusion enhancement [47]. The gliding GB dislocations (resulting from the splitting of trapped dislocations) carry GB sliding which leads to the formation of superdislocations at triple junctions (Fig. 1). The stresses created by the superdislocations are relaxed via either the nanocrack generation or enhanced GB diffusion in the vicinity of these junctions. If the former mechanism for stress relaxation is dominant, intense generation and convergence of triple junction nanocracks result in the brittle behavior of a nanocrystalline specimen. If the second relaxation mechanism is dominant, the nanocrack generation is suppressed in a deformed nanocrystalline specimen which therefore is able of exhibiting a good ductility or even superplasticity.

In the context discussed, of particular interest are experimental data [7,48] on observations of both grain rotation and GB sliding simultaneously occurring in deformed nanocrystalline materials. Grain rotation occurs in nanocrystalline materials when it is effectively accommodated by enhanced diffusion along GBs [49]. In these circumstances, experimental observation [7,48] of grain rotation in nanocrystalline materials under plastic and superplastic deformation regimes is indicative of the enhanced GB diffusion processes in these materials. At the same time, cracks have not been experimentally observed in these materials [7,48]. Thus, experimental data [7,48] indicate that both GB sliding and GB diffusion occur in deformed nanocrystalline materials without crack nucleation. These experimental data support our model which naturally explains them as follows. GB sliding occurs but does not induce nanocrack nucleation in deformed nanocrystalline materials, because GB diffusion provides its effective suppression.

In addition, the suggested model is indirectly supported by the experimental data [2] on degradation of superplastic properties of nanocrystalline materials after a short thermal treatment. More precisely, Islamgaliev et al. [2] reported that nanocrystalline materials fabricated by severe plastic deformation method and then subjected to a short heat treatment do not show superplastic behavior, in contrast to as-fabricated materials. In the experiment [2], heat treatment is not enough intense to cause grain growth but is sufficient to induce annihilation of the non-equilibrium GB vacancies generated in nanocrystalline materials during their fabrication by severe plastic deformation. In terms of our model, after heat treatment, the density of GB vacancies abruptly decreases and thereby the GB diffusion (occurring mostly by GB vacancy transport) becomes a low-intensity process which is not able of suppressing the nanocrack nucleation. As a result, though a nanocrystalline specimen in its as-fabricated state shows superplasticity, heat treatment leads to its dramatic degradation.

Finally, notice that the role of the lattice dislocation slip in nanocrystalline materials diminishes with decreasing the grain size. Such deformation mechanisms as Coble creep [50–52] and triple junction diffusional creep [53] are capable of essentially contributing to plastic flow in nanocrystalline materials with the finest grains. In these materials, where the lattice dislocation slip does not operate, deformation and fracture processes can occur in a different way compared to the case described in this paper.

Acknowledgments

This work was supported, in part, by the Office of US Naval Research (Grant N00014-01-1-1020), INTAS (Grant 03-51-3779), the Russian Science Support Foundation, St. Petersburg Scientific Center, and RAS Program "Structural Mechanics of Materials and Construction Elements".

References

[1] McFadden SX, Mishra RS, Valiev RZ, Zhilyaev AP, Mukherjee AK. Nature 1999;398:684.
[2] Islamgaliev RK, Valiev RZ, Mishra RS, Mukherjee AK. Mater Sci Eng A 2001;304–306:206.
[3] Mishra RS, Valiev RZ, McFadden SX, Islamgaliev RK, Mukherjee AK. Philos Mag A 2001;81:37.
[4] Mishra RS, Stolyarov VV, Echer C, Valiev RZ, Mukherjee AK. Mater Sci Eng A 2001;298:44.
[5] Valiev RZ, Song C, McFadden SX, Mukherjee AK, Mishra RS. Philos Mag A 2001;81:25.
[6] Valiev RZ, Alexandrov IV, Zhu YT, Lowe TC. J Mater Res 2002;17:5.
[7] Mukherjee AK. Mater Sci Eng A 2002;322:1.
[8] Zhan G-D, Kuntz JD, Wan J, Mukherjee AK. In: Berndt CC, Fischer T, Ovid'ko IA, Skandan G, Tsakalakos T, editors. Nanomaterials for structural applications. MRS symposium proceedings, vol. 740. Warrendale: MRS; 2003. p. 41.
[9] Pilling J, Ridley N. Superplasticity in crystalline solids. London: The Institute of Metals; 1989.

[10] Mohamed FA, Li Y. Mater Sci Eng A 2001;298:1.
[11] Kumar KS, Suresh S, Swygenhoven H. Acta Mater 2003;51:5743.
[12] Koch CC, Morris DG, Lu K, Inoue A. MRS Bull 1999;24:54.
[13] Jia D, Ramesh KT, Ma E. Acta Mater 2003;51:3495.
[14] Kumar KS, Suresh S, Chisholm MF, Horton JA, Wang P. Acta Mater 2003;51:387.
[15] Champion Y, Lahglois C, Guerin-Mailly S, Langlois P, Bonnentien J-L, Hytch M. Science 2003;300:310.
[16] Wang Y, Chen M, Zhou F, Ma E. Nature 2002;419:912.
[17] He G, Eckert J, Loeser W, Schultz L. Nat Mater 2003;2:33.
[18] Ke M, Hackney SA, Milligan WW, Aifantis EC. Nanostruct Mater 1995;5:689.
[19] Gutkin MYu, Kolesnikova AL, Ovid'ko IA, Skiba NV. Philos Mag Lett 2002;81:651.
[20] Gutkin MYu, Ovid'ko IA, Skiba NV. Acta Mater 2003;51:4059.
[21] Ovid'ko IA. Science 2002;295:2386.
[22] Murayama M, Howe JM, Hidaka H, Takaki S. Science 2002;295:2433.
[23] Gutkin MYu, Ovid'ko IA. Plastic deformation in nanocrystalline materials. Berlin: Springer; 2004.
[24] Gutkin MYu, Ovid'ko IA, Skiba NV. J Phys D 2003;36:L47.
[25] Gutkin MYu, Ovid'ko IA, Skiba NV. Acta Mater 2004;52:1711.
[26] Ovid'ko IA, Sheinerman AG. Acta Mater 2004;52:1201.
[27] Ovid'ko IA, Sheinerman AG. Rev Adv Mater Sci 2004;7:61.
[28] Farkas D, Van Swygenhoven H, Derlet PM. Phys Rev B 2002;66:060101.
[29] Morozov NF, Ovid'ko IA, Petrov YuV, Sheinerman AG. Rev Adv Mater Sci 2003;4:65.
[30] Sutton AP, Balluffi RW. Interfaces in crystalline materials. Oxford: Oxford Science Publications; 1996.
[31] Hirth JP, Lothe J. Theory of dislocations. New York: Wiley; 1982.
[32] Gleiter H. Prog Mater Sci 1989;33:223.
[33] Evans AG, Rice JR, Hirth JP. J Am Ceram Soc 1980;63:368.
[34] Raj R, Ashby MF. Metall Trans 1971;2:1113.
[35] Timoshenko SP, Goodier JN. Theory of elasticity. New York: McGraw-Hill; 1970.
[36] Chuang T-J, Kagawa KI, Rice JR, Sills LB. Acta Metall 1979;27:265.
[37] Indenbom VI. Fiz Tverd Tela 1961;3:2071. [Trans. in Sov Phys Solid State].
[38] Rybin VV, Zhukovskii IM. Phys Tverd Tela 1978;20:1829. [Trans. in Sov Phys Solid State].
[39] Vladimirov VI, Gutkin MYu, Romanov AE. Mech Compos Mater 1987;23:313.
[40] Gutkin MYu, Ovid'ko IA. Philos Mag A 1994;70:561.
[41] Smithells CJ, Brands EA. Metals reference book. London: Butterworth; 1976.
[42] Nazarov AA. Phys Solid State 2003;45:1166.
[43] Ma E. Scr Mater 2003;49:663.
[44] Hahn H, Padmanabhan KA. Philos Mag B 1997;76:559.
[45] Konstantinidis DA, Aifantis EC. Nanostruct Mater 1998;10:1111.
[46] Fedorov AA, Gutkin MYu, Ovid'ko IA. Acta Mater 2003;51:887.
[47] Ovid'ko IA, Sheinerman AG. Philos Mag 2003;83:1551.
[48] Chan Z, Stach EA, Wiezorek JMK, Knapp JA, Follstaedt DM, Mao SX. Science 2004;305:654.
[49] Moldovan D, Wolf D, Phillpot SR. Acta Mater 2001;49:3521.
[50] Masumura RA, Hazzledine PM, Pande CS. Acta Mater 1998;46:4527.
[51] Masumura RA, Pande CS. In: Berndt CC, Fischer T, Ovid'ko IA, Skandan G, Tsakalakos T, editors. Nanomaterials for structural applications. MRS symposium proceedings, vol. 740. Warrendale: MRS; 2003. p. 3.
[52] Yamakov V, Wolf D, Phillpot SR, Gleiter H. Acta Mater 2002;50:61.
[53] Fedorov AA, Gutkin MYu, Ovid'ko IA. Scr Mater 2002;47:51.